


53.301-298

AD-A252 296

FEDERAL ACQUISITION REGULATION (FAR)

		1 PAGE		Form Approved OMB No 0704-0188	
<small>For per response, including the time for reviewing instructions, searching existing data sources, gathering of information. Send comments regarding this burden estimate or any other aspect of this form on Headquarters Services, Directorate for Information Operations and Reports, 1215 Jefferson Avenue and Budget, Paperwork Reduction Project (0704-0188), Washington, DC 20503.</small>					
1. AGENCY USE ONLY (Leave blank)		2. REPORT DATE 4/92		3. REPORT TYPE AND DATES COVERED final 7/1/89 - 12/31/91	
4. TITLE AND SUBTITLE Sources of Anisotropy in Amorphous Magnetic Thin Film				5. FUNDING NUMBERS AFOSR-89-0432	
6. AUTHOR(S) Dr. Frances Hellman					
7. PERFORMING ORGANIZATION NAME(S) AND ADDRESS(ES) Department of Physics, 0319 University of California, San Diego 9500 Gilman Drive La Jolla, CA 92093-0319				8. PERFORMING ORGANIZATION REPORT NUMBER AFOSR-TR 82 0523	
9. SPONSORING/MONITORING AGENCY NAME(S) AND ADDRESS(ES) AFOSR/NE Building 410 Bolling AFB, DC 20332-6448 <i>Wierstock</i>				10. SPONSORING/MONITORING AGENCY REPORT NUMBER 2306/CI	
11. SUPPLEMENTARY NOTES					
12a. DISTRIBUTION/AVAILABILITY STATEMENT no limitation				12b. DISTRIBUTION CODE	
13. ABSTRACT (Maximum 200 words) Macroscopic magnetic anisotropy is induced in the amorphous rare earth-transition metal alloys such as Tb-Fe when they are prepared by vapor deposition processes. The role of the vapor deposition process in producing the structural anisotropy which underlies the magnetic anisotropy has been explored and results compared with proposed models. It was shown that the anisotropy is independent of the state of stress in the film during the growth, and does not depend on film thickness, results inconsistent with recently-proposed models. Most significantly, the anisotropy was shown to be induced by a <u>thermally-activated</u> growth process. This process was hypothesized to involve rearrangement of local adatom configurations into energetically-favorable orientations which minimize surface energy during the growth, a process analogous to the frequently-observed crystallographic texturing of polycrystalline thin films. The anisotropy vanishes upon subsequent annealing of the films, emphasizing the critical role of the surface					
14. SUBJECT TERMS during growth.				15. NUMBER OF PAGES 10	
				16. PRICE CODE n/a	
17. SECURITY CLASSIFICATION OF REPORT UNCLASSIFIED		18. SECURITY CLASSIFICATION OF THIS PAGE UNCLASSIFIED		19. SECURITY CLASSIFICATION OF ABSTRACT UNCLASSIFIED	
				20. LIMITATION OF ABSTRACT UL	

NSN 7540-01-280-5500

Standard Form 298 (Rev 2-89)
Prescribed by ANSI Std Z39-18
298 102

AFOSR FINAL REPORT: F. Hellman, University of California, San Diego

#89-0432: 7/1/89-12/31/91

ABSTRACT

Macroscopic magnetic anisotropy is induced in the amorphous rare earth-transition metal alloys such as Tb-Fe when they are prepared by vapor deposition processes. The role of the vapor deposition process in producing the structural anisotropy which underlies the magnetic anisotropy has been explored and results compared with proposed models. It was shown that the anisotropy is independent of the state of stress in the film during the growth, and does not depend on film thickness, results inconsistent with recently-proposed models. Most significantly, the anisotropy was shown to be induced by a *thermally activated* growth process. This process was hypothesized to involve rearrangement of local adatom configurations into energetically-favorable orientations which minimize surface energy during the growth, a process analogous to the frequently-observed crystallographic texturing of polycrystalline thin films. The anisotropy vanishes upon subsequent annealing of the films, emphasizing the critical role of the surface during growth.

This model for vapor deposition growth of the amorphous phase is quite novel; further work currently being pursued (structural and thermodynamic as well as magnetic measurements on different alloys) will confirm or contradict it. In particular, the importance of the surface energy during growth and the existence of a fairly-well defined deposition temperature at which the properties of the amorphous phase change dramatically are factors analogous to those found crucial to growth of high quality *crystalline* alloys. It is not obvious how to extend the concept of a close-packed low energy surface to the *amorphous* phase, but the results suggest that this is the correct way of viewing it.

92-15739



Accession For	
NTIS GRA&I	<input checked="" type="checkbox"/>
DTIC TAB	<input type="checkbox"/>
Unannounced	<input type="checkbox"/>
Justification	
By	
Distribution/	
Availability Codes	
Dist	Avail and/or Special
A-1	

92 6 16 097

RESULTS

1. Amorphous phase texturing and perpendicular anisotropy

When amorphous Tb-Fe (and other rare earth-transition metal alloys) are prepared by vapor deposition processes, they have long been known to possess a large uniaxial magnetic anisotropy normal to the film plane. This anisotropy is critical to the materials' current use in magneto-optic recording, a relatively novel, high bit-density and access rate, non-volatile, robust, read-write-erase storage technology. The role of the vapor-deposition process and the structural origin of a macroscopic anisotropy in an amorphous material is still, however, not understood. A number of different sources of the structural anisotropy underlying the magnetic anisotropy have been postulated, ranging from stress, to a columnar microstructure, to a chemical or topological short range order which becomes oriented normal to the film due to some generally-unspecified vapor-deposition process. Recent suggestions have included a *surface* anisotropy of magnetic dipolar origin (implying that the anisotropy would vary as the inverse film thickness) and a growth-induced anisotropy due to magnetic interactions of all subsequently-deposited layers with a perpendicularly-magnetized first layer (an effect which must vanish above T_c). Relatively recent x-ray observations of a compressive strain apparently far larger than was consistent with the measured elastic stress prompted a theory that the anisotropy was due to an "anelastic strain", due to stress at the surface during growth distorting the local structure and leaving a permanent *anelastic* effect (in addition to the elastic strain).

We have, however, recently shown that the perpendicular anisotropy is independent of the sign of the stress during growth, a result inconsistent with the anelastic strain model. We have also shown that the anisotropy is independent of sample thickness and *increases* with increasing deposition temperature, including temperatures far above the Curie temperature. The non-randomness in the amorphous phase is therefore not due to magnetic interactions nor kinetic effects of vapor-deposition growth, such as shadowing and incident atomic beam directions, which are reduced by raising the deposition temperature. Fig.1 shows the most significant result we obtained: the magnitude of the anisotropy of $a\text{-Tb}_x\text{Fe}_{100-x}$ as a function of deposition temperature for tensile and compressive films (solid and open symbols respectively). We have found that neither the remanent moment (in zero field) nor T_c are significantly affected by deposition temperature, implying that no dramatic changes in the local structure are occurring, only a subtle alignment of the local environments around the Tb ions. We have also found that annealing (2 hrs. at 620K, *below* the highest deposition temperature shown) eliminates the anisotropy, as also observed by others, strongly suggesting that the anisotropy is not due to formation of small microcrystallites. Furthermore, $a\text{-Tb-Fe}$ (with a large macroscopic anisotropy) has been one of the most extensively studied materials by x-ray scattering, neutron scattering, EXAFS, Mossbauer, and TEM, and no sign of microcrystallites was ever observed.

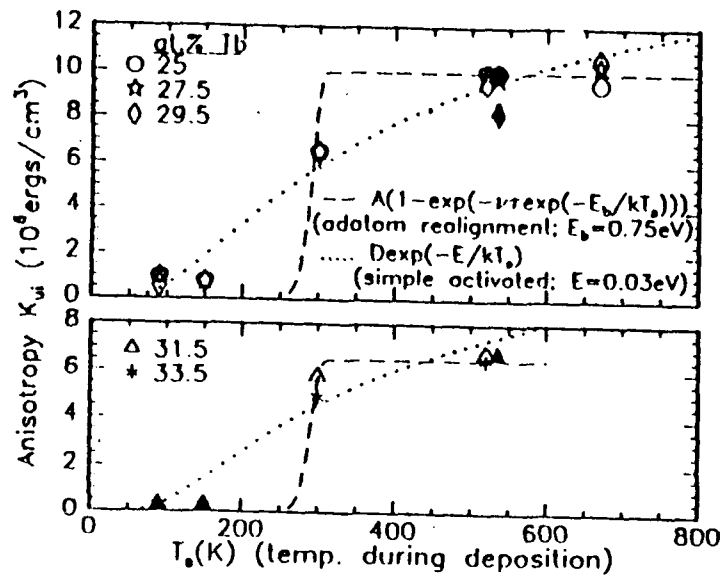


Fig. 1 Macroscopic anisotropy measured at room temperature vs deposition temperature T_s of 5000 Å thick $a\text{-Tb}_x\text{Fe}_{100-x}$. Open symbols: Ar pressure during growth $5 \mu\text{m}$; films in compression at T_s . Solid symbols: Ar pressure $10 \mu\text{m}$; films in tension at $T_s = 520 \text{ K}$ (data shown at 535 K for clarity). Lines show fits, as described in text.

We have suggested (Phys. Rev. Lett. 3/2/92) that these various observations of the macroscopic anisotropy are explained by considering the source to lie in a phenomenon we called "texturing", analogous to texturing of the crystallographic orientations in vapor-deposited polycrystalline materials. We have also suggested that this process involves a rearrangement of local adatom configurations into energetically-favorable orientations which minimize surface energy during growth, an effect previously proposed to explain the deposition temperature dependence of various (isotropic) properties of $a\text{-Ge}$. These local structures possess a local anisotropy, and hence their alignment in some preferred orientation will cause a macroscopic magnetic anisotropy. Once any given surface layer is buried by the next layer of incoming atoms, all directions become equivalent. The anisotropic local structure is however frozen in by low bulk diffusion rates; it may then be eliminated only by long-time annealing. This process is thus one which relies on a surface local equilibrium.

Figure 1 shows fits to the above-described adatom re-orienting model and to a generic, thermally-activated process. The energy barrier for re-orienting is a reasonable one (given the data for $a\text{-Ge}$). The activation energy found by fitting the data to a generic thermally-activated process is very low (compared for example to typical surface diffusion values).

EXAFS analysis and x-ray scattering work is currently in progress to look for direct structural evidence of the anisotropy (in collaboration with V. Harris at NRL and A. Bienenstock, director of the Stanford Synchrotron Radiation Lab, respectively).

2. Stochastic kinetic model of vapor-deposition growth

A specific model for a growth-surface-induced, thermally-activated anisotropy was the commonly-heard theory that a non-zero energy of mixing of an AB alloy would lead to an anisotropic distribution of AB pairs versus AA and BB. Specifically, since an adatom of type A would preferentially occupy sites with more type-B neighbors in the layer below, as the material grows, A-B pairs would tend to form vertically. Such a model might be expected to give a thermally-activated behavior; at low temperatures, adatoms will be trapped by the potential well at virtually any site while at higher temperatures, thermal energy will allow it to escape from the shallower wells involving like-neighbors but still remain trapped in the deeper wells with many-unlike neighbors. (The essence of this argument is shown schematically in Fig. 2). In order to model these purely *chemical* effects on the growth of amorphous alloys, using realistic deposition rates relative to surface diffusion, we developed a stochastic, kinetic model for growth of chemically-disordered, structurally-ordered binary alloys (paper in preparation). The results for an fcc A_3B alloy grown in the (100) direction are shown in Fig. 3. With increasing deposition temperature, increasing short range order forms, until an upper temperature where thermal energy exceeds the energy of mixing. However, *no anisotropic short range order* is found at any deposition temperature. Related results are found for all deposition rates. Our results suggest that a simple energy of mixing alone is insufficient to produce the magnetic anisotropy in the amorphous alloys, leading us back to a more subtle texturing model, as discussed above.

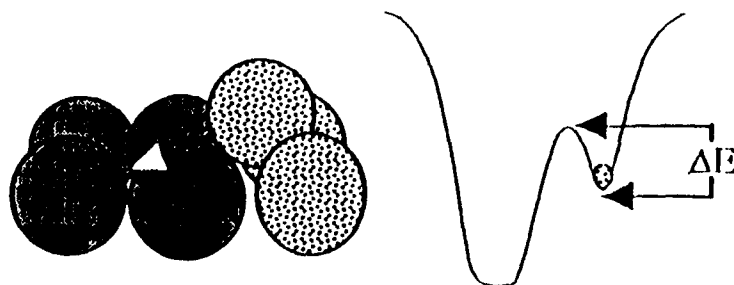


Fig. 2 Stochastic kinetic growth (SKS) model of (100)-oriented growth of fcc A-B alloy. Mobile surface atom moves into nearest neighbor vacancy. The barrier crossing rate is given by $\Gamma = \nu \exp(-\Delta E/kT)$ where ΔE is the height of the kinetic barrier separating the mobile atom from the vacant site. ΔE is a function of the occupation of the 12 nearest neighbors to each site (empty, A-occupied, or B-occupied).

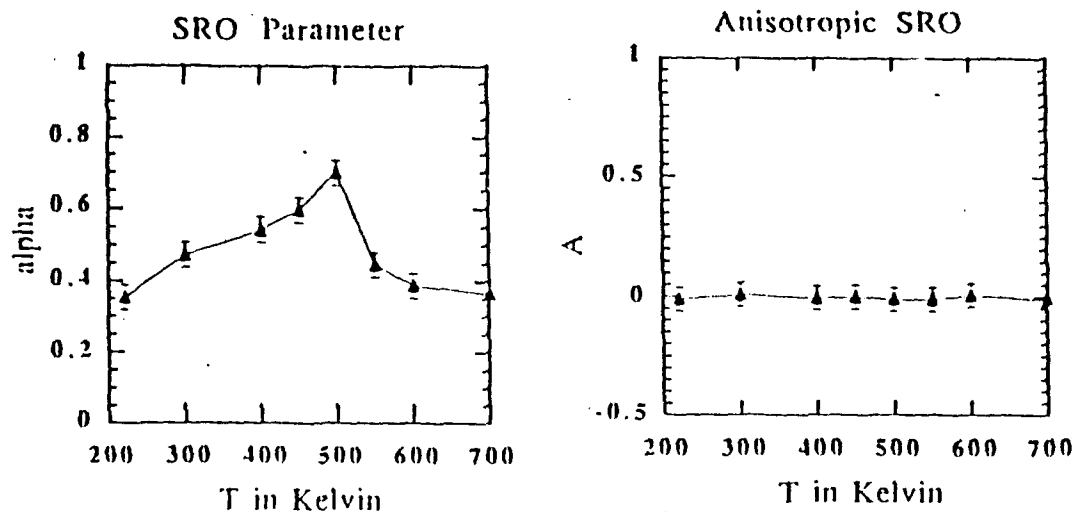


Fig. 3 a) Short range order parameter α as a function of deposition temperature in SKS simulation for a particular deposition rate. (α is the Warren-Cowley parameter normalized by the value for a perfectly-ordered A_3B alloy: .33). At 500K, thermal energy is equal to the heat of mixing ϵ of the A-B alloy. **b)** Anisotropic short range order parameter A = number of A-B bonds out of plane/number of A-B bonds in plane.

c) Thermodynamic measurements

We have built a system capable of measuring the thermodynamic properties of thin films from 1K to room temperature. The microcalorimeters upon which the measurements depend are capable of measurements up to 1100K. They have two orders of magnitude less addenda than any other thin film system at all temperatures. These devices make possible measurements of thin film samples less than 100 Å thick (weighing less than 1 µg) below 10K and 1000-5000 Å thick (weighing 10-50 µg) up to 1100K. These capabilities are quite unique. The microcalorimeters consist of a thin (1800 Å) .5 x .5 cm² amorphous Si₃N₄ membrane. On one side of this membrane, we deposit and pattern thin film heater, thermometers, and electrical leads of appropriate resistance and temperature coefficient. On the other side, in a .25 x .25 cm² area at the center, we deposit the sample. The membrane is supported by a 1 x 1 cm² Si frame. On the frame are matching thermometers to those on the membrane to permit a high sensitivity differential temperature measurement. Fig. 4a) (next page) shows a superposition of the photolithographic masks used to make the devices and 1b) a photograph of a device with a sample. We currently have several dozen of these devices with gold, aluminum, and copper samples on the back for testing and calibration purposes. The devices are metallurgically stable and physically robust under cycling between 4.2K and 1000K, and can withstand photolithographic processing, being dropped (most of the time), or handling with tweezers. The preferred method of sample preparation is to deposit the sample through an evaporation mask which fits down into the etched pit, close to the membrane, but samples have been also defined by photolithographic processing.

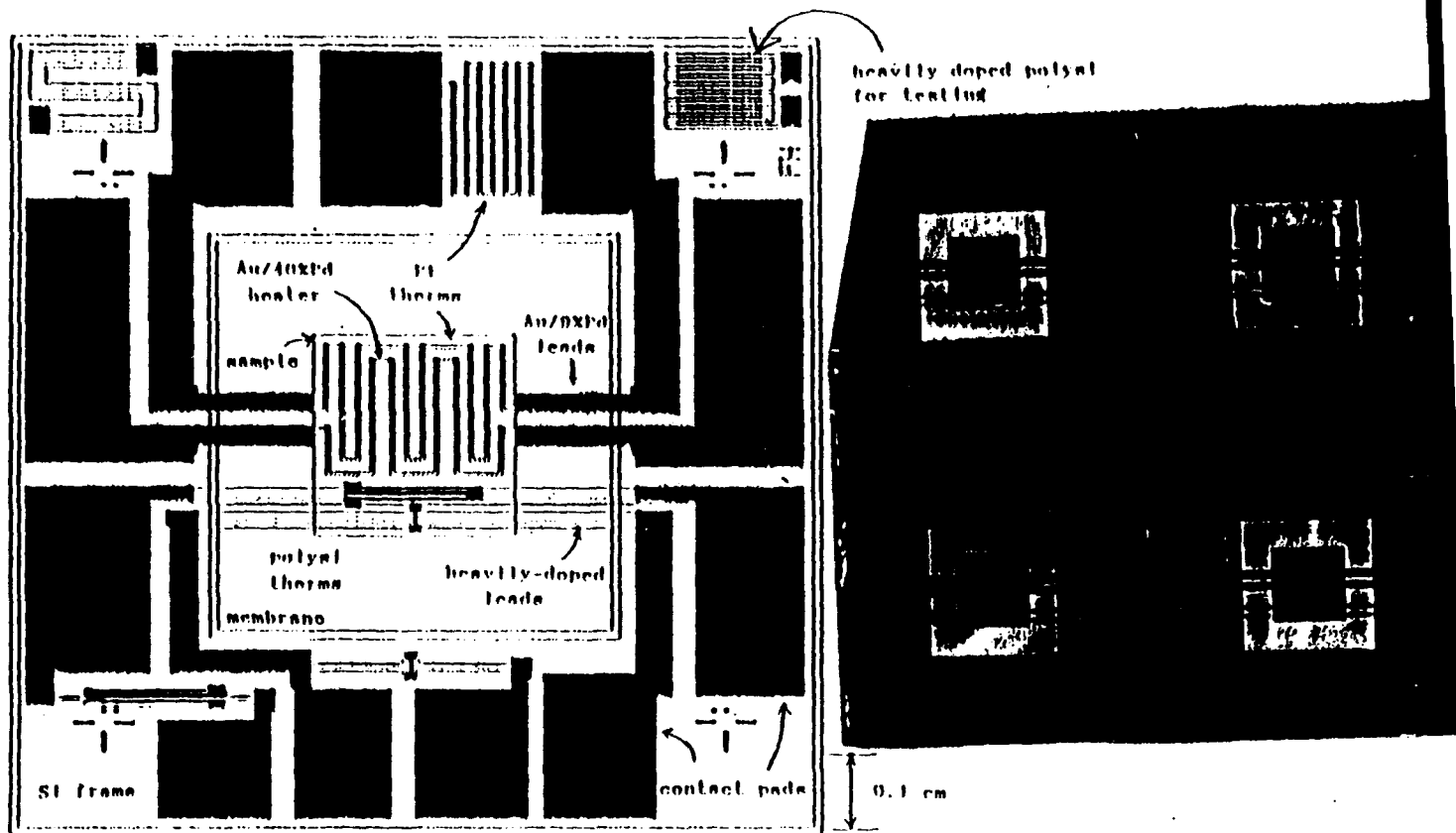


Fig. 4 a) Schematic overlay of photolithographic masks used to make microcalorimeters. b) Photograph of microcalorimeters with 1800Å gold sample on backside of membrane.

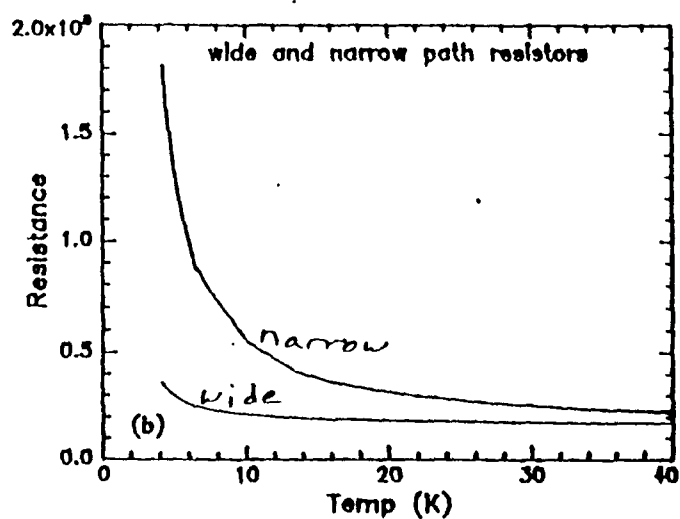
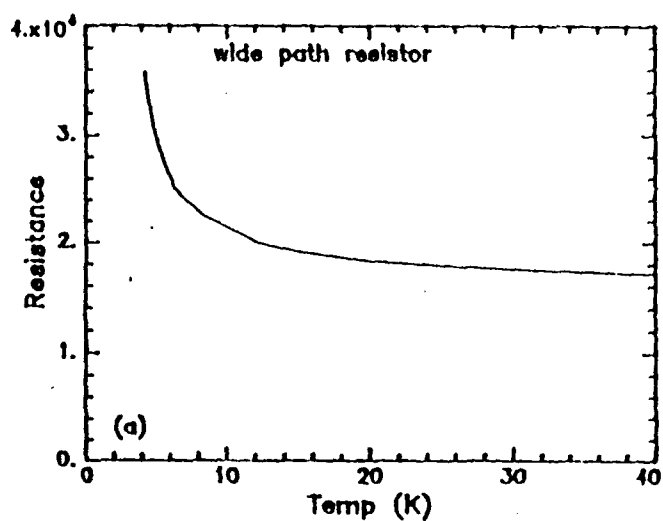


Fig. 5 Resistivity of polysil thermometers: a) wide path resistor (for 1-20K) b) narrow path resistor (same doping) (4-40K), compared to wide path, expanded scale.

Requirements of sensitivity at low temperatures and metallurgical stability at high temperature (and the need to grow it on a membrane) caused us to develop a new low T thermometer: doped polycrystalline Si (polysi), about which nothing previously was known below 77K. We have developed a process for making ion-implanted polysi with heavily doped polysi leads and Ti contacts, buried inside a Si_3N_4 membrane "sandwich". Since they are annealed at 1300K during processing, we do not expect metallurgical problems at the anticipated upper limit of 1100K. Plots of resistivity of the two low T thermometers (differing in their useful temperature ranges due solely to path widths) are shown in Fig. 5 (previous page).

Results are shown in Fig. 6 for two gold samples and the calorimeter addenda from 77-300K. Calibrations at low temperatures are currently being made. Two papers concerning this work are in progress: one on the microcalorimeters and one on the new polysi thermometers.

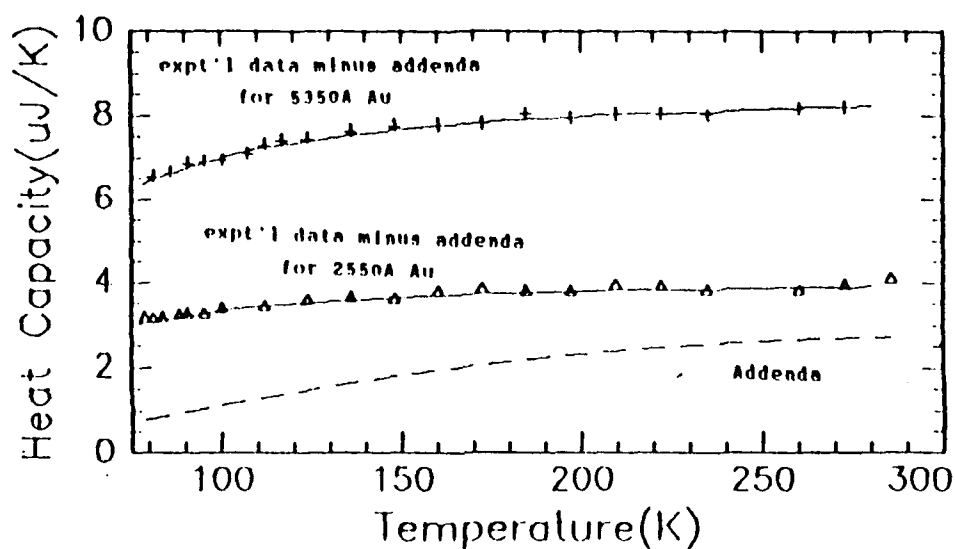


Fig. 6 Heat capacity of 2500Å and 5800Å gold samples and microcalorimeter addenda (dashed line). Solid lines-expected heat capacity.

During the course of the work on magnetic anisotropy in amorphous thin films, we have constructed several pieces of necessary equipment. Our most unique work is the fabrication of the world's most sensitive microcalorimeters, described above. We have also put together a vibrating sample magnetometer and a torque magnetometer for measuring the magnetic properties of these alloys, and a high vacuum magnetic annealing furnace to test crystallizing of the amorphous alloys.

d) Vortices in superconductors

Using the magnetometers constructed under this proposal, we have investigated the effect of applying a magnetic field at an angle to both intrinsically isotropic and anisotropic superconductors. We found some very unexpected results for isotropic materials with a

relatively small shape anisotropy only. Specifically, the induced magnetization lies nearly perpendicular to a parallelepiped sample with an aspect ratio of only 2:1 and the applied field at up to a 45 degree angle. We are currently extending this work to anisotropic superconductors.

Future work

We will continue our investigations into the cause of the vapor-deposition induced magnetic anisotropy and more generally into the effect of the vapor deposition process on the amorphous structure. We will also investigate a predicted crossover from a disordered spin-glass-like state to a magnetically-ordered (ferro- or ferri- magnetic) state with increasing K_{ui} , using the full range of thermodynamic and magnetic measurements. Measurements will be compared with direct imaging of domains using newly-developed magnetic imaging techniques (such as the near field microscope or the magnetic force microscope). High field transport measurements (Hall effect and magnetoresistance in a magnetic field parallel or perpendicular to the current) and Mossbauer measurements provide complementary information. Our unique microcalorimeters mean that we can for the first time make thermodynamic measurements on thin films; the specific heat through T_f (divergent for a ferromagnetic state and broad and frequency and field-dependent for the spin glass-like state) is a powerful characterization tool. The magnetic entropy up through T_f is also an important characterization both of the local "crystal" fields and of the extent of magnetic short range order still existing at temperatures above T_f . The thermodynamic and magnetic measurements made possible under this grant make such work possible.

The technologically-important and scientifically-interesting problem of the coercivity in these materials (e.g. α -Tb-Fe) and its dependence both on random local anisotropy and on the magnitude of the macroscopic anisotropy will also be investigated. Initially, we will explore the long time scale coercive field using dc magnetization hysteresis loops, but if measurements prove interesting, we will also investigate time dependent effects.

The reactivity of the rare earths require attention to avoid oxidation. Samples will be prepared in a UHV multi-source electron beam evaporator. For most purposes, they may be coated with a protective overlayer and then removed from the vacuum. For cases where this is impossible (e.g. deposition at low temperatures where annealing would occur even at room temperature, or for high temperature annealing studies where reactions with an overlayer might cause difficulty), we will use a UHV-compatible LHe dewar which we have recently designed with Janis Research, Inc. (from 1.5K to ~500K) or a more traditional UHV furnace/LN₂ sample platform (from ~150K up to 1100K) to allow us to measure specific heat, susceptibility, and resistivity *in situ*.

The continuing work on understanding the growth of the amorphous phase by vapor deposition consists of several components. 1) We are testing the adatom re-orientation model (see Fig. 1 and accompanying text) by varying the deposition rate at fixed deposition temperature and by looking at other amorphous alloys. 2) We are currently exploring ways to extend our stochastic kinetic growth model to include size effects, bringing it a step closer to modeling growth of the amorphous phase. 3) We will explore the use of high temperature (to 800°C) thermodynamic measurements (the enthalpy release up through either the glass transition or crystallization) to determine the excess structural enthalpy for samples of the same composition prepared for example at different deposition temperatures. This excess enthalpy is an indirect measurement of the as-deposited amorphous structure. High temperature thermodynamic measurements will also help distinguish between microcrystalline and truly amorphous structures. 4) Direct structural analysis is being explored to see if differences in the as-grown amorphous structure can be resolved. Measurements of density will also be made (by comparing Rutherford back-scattering measurements or sample weight with thickness determinations) for films grown at different deposition temperatures before and after annealing. 5) We are exploring the vapor-deposition growth of amorphous alloys by growing them on either an amorphous substrate or on a crystalline underlayer of the sample's composition (prepared for example by prior annealing) and determining the minimum deposition temperature for crystalline growth when nucleation sites are present compared to when they are not. Growth of crystalline and amorphous Si on ordered and disordered substrates does indeed support a model of nucleation-site-limiting, but tests on metallic alloys have, to the best of our knowledge, not yet been performed. 6) We will compare materials of the same composition but with different thermal history to see if the *magnetic* correlation lengths depend on thermal history in a way that can be sensibly associated with structural short range order.

PAPERS (in refereed journals)

1. F. Hellman, "Measurement of magnetic anisotropy of ferrimagnets near compensation". Appl. Phys. Lett. **59**, 2757 (1992).
2. F. Hellman, E. M. Gyorgy, and R. C. Dynes, "Quasi-2D behavior in bulk isotropic type II superconductors: shape effects". Phys. Rev. Lett. **68**, 867 (1992).
3. F. Hellman and E. M. Gyorgy, "Growth-Induced Magnetic Anisotropy in Amorphous Tb-Fe". Phys. Rev. Lett. **68**, 1391 (1992).
4. J. K. Trautman, E. Betzig, J. S. Weiner, D. J. DiGiovanni, T. D. Harris, F. Hellman, and E. M. Gyorgy, "Image contrast in near-field optical microscopy: demonstrating a versatile technique beyond the diffraction limit". J. Appl. Phys.

5. P. W. Rooney and F. Hellman, "A Kinetic Simulation of Vapor Deposition and Growth." (In preparation: to be submitted to Phys. Rev. B).
6. F. Hellman, "High-Field Susceptibility of Amorphous Tb_xFe_{1-x} ; a Re-Examination of the Random Magnetic Anisotropy model". (In progress: to be submitted to Phys. Rev. Lett.)
7. F. Hellman and E. M. Gyorgy, "Increased Coercive Force and Decreased Anisotropy in Amorphous Tb_xFe_{1-x} Prepared at Low Substrate Temperature". (In progress: to be submitted to Appl. Phys. Lett.)
8. F. Hellman, E. M. Gyorgy, and R. J. Felder, "Anomalies in the Composition Dependence of the Magnetic Anisotropy of Amorphous Tb-Fe and Ho-Fe". (To be submitted to Phys. Rev. B).

Conference presentations:

1. F. Hellman, E. M. Gyorgy, R. B. van Dover, and R. J. Felder, "Anomalous Composition Dependence of Anisotropy in Amorphous Tb-Fe and Ho-Fe." Proceedings of the 35th conference on Magnetism and Magnetic Materials, Nov. 1990.
2. F. Hellman, E. M. Gyorgy, and R. C. Dynes, "Vortex Structure and Macroscopic Screening in Superconducting Slabs and Films in Oblique Magnetic Fields." March 1991 meeting of the APS.
3. F. Hellman, "High-field susceptibility of amorphous Tb_xFe_{1-x} ; a Re-examination of the Random Magnetic Anisotropy Model." March 1991 A.P.S. Meeting.
4. F. Hellman, E. M. Gyorgy and R. J. Felder, "Evidence for Surface-Mediated Amorphous Phase Texturing as Source of Perpendicular Anisotropy in α -Tb-Fe." 1991 Spring Meeting, MRS.
5. P. W. Rooney and F. Hellman, "Kinetic Growth Simulation of a Binary Metallic Alloy with a Positive Heat of Mixing." 1991 Spring Meeting, MRS.
6. F. Hellman, (Invited), "Vapor-deposition-induced magnetic anisotropy in amorphous RE-TM alloys", Magnetism and Magnetic Materials Conference, Pittsburgh, July 1991.
7. P. W. Rooney and F. Hellman, "A Kinetic Simulation of Vapor Deposition and Growth." March 1992 APS Meeting.